Porous Coordination Networks

DOI: 10.1002/ange.201306776

Kinetic Assembly of a Thermally Stable Porous Coordination Network Based on Labile CuI Units and the Visualization of I_2 Sorption**

*Hakuba Kitagawa, Hiroyoshi Ohtsu, and Masaki Kawano**

The advantage of porous coordination network synthesis is the control of design that is possible by changing the metal sources and ligands.[1] Therefore, not only many commercially available ligands but also newly synthesized ones have been used for preparing coordination networks.[2] In contrast most of the metal sources employed are common reagents or stable metal moieties because their behavior as a metal connector is predictable. To date, to our knowledge, there is no report focusing on use of labile metal sources for selective network formation. One of the promising methods to produce unique networks with such labile metal sources is kinetic control, which has been used for long time to prepare various other sorts of materials.[3] Herein we report the first selective syntheses of thermally stable porous coordination networks using a labile Cu_4I_4 cubane cluster and a rigid T_d-symmetry ligand by both kinetic and thermodynamic control. Although the CuI readily produces a mixture of several kinds of coordination compounds containing a Cu_4I_4 cubane or a Cu_2I_2 dimer unit,[4] we succeeded in kinetically and selectively preparing porous network crystals composed of novel CuI helical chains which can keep their crystallinity up to 673 K under N_2 atmosphere. Because I_2 sorption by porous compounds has significant potential, for example, as a nuclear fission product absorber,[5] we tested I_2 encapsulation into the pores of the network. The network crystals show chemisorption of I_2 by formation of a covalent bond with an iodide of part of the framework to form an I_3^- group. As the thermodynamic product, we obtained a Cu_2I_2 dimer network which shows physisorption of I_2. We confirmed these different processes in solution by kinetic measurements. We also demonstrated the mechanism of network formation in this system by NMR spectroscopy.

We chose a compound having a Cu_4I_4 cubane core, $[Cu_4I_4(PPh_3)_4]$ (**1**), as a labile metal source to demonstrate our concept, because a Cu_4I_4 cubane core can be converted readily into other CuI units in the solution state even though it is stable in the solid state.[4,6] For the rigid ligand, we prepared a thermally stable T_d-symmetry tetradentate ligand (tetra-4-(4-pyridyl)phenylmethane, **2**) (Scheme 1, see Figure S3 in the Supporting Information, for further information on stability).[7] On heating of the mixture of the labile metal source

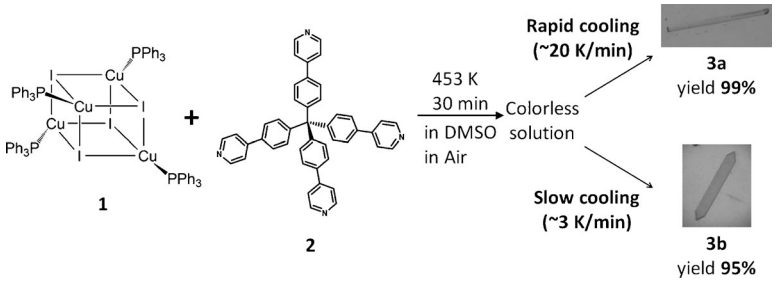

Scheme 1. Selective preparation of network isomers **3a** and **3b**.

1 and ligand **2** in DMSO in air at 453 K, a homogenous colorless solution was obtained. By cooling this solution, two kinds of network crystals were obtained. Because the ratio of the two crystals changed depending on the cooling rate, we assumed that this result is attributed to kinetic/thermodynamic effects. (Details are described in Supporting Information). As we expected, rapid cooling (ca. 20 K min^{-1}) produced exclusively yellow needle crystals, $\{[(CuI)_2(\mathbf{2})]\cdot solvent\}_n$ (network isomer **3a**), in 99% yield. On the other hand, slow cooling (ca. 3 K min^{-1}) produced orange prism crystals, $\{[(Cu_2I_2)(\mathbf{2})]\cdot solvent\}_n$ (network isomer **3b**), in 95% yield. These two networks have the same molecular formula, however show different connectivity as discussed below.

The crystal-structure analysis of isomer **3a** revealed that along the *c* axis CuI helical chains bridged by ligand **2** form a non-interpenetrated porous network in which a Cu^I ion is coordinated by two N atoms of ligand **2** and two iodides (Figure 1 a,c, and e).[8] The helical chain network isomer **3a** has 1D channels with the pore window of 5.8 × 5.5 Å and 35% void space (without solvent) in the unit cell volume. The salient feature of this network structure is that the bridging iodide in the framework faces into the 1D channel.

The crystal structure analysis of isomer **3b** revealed that isomer **3b** is a quadruply interpenetrated network consisting of Cu_2I_2 dimer units and ligand **2** (Figure 1 b,d, and f; and see Figure S4 in the Supporting Information). The network is

[*] H. Kitagawa, Dr. H. Ohtsu, Prof. Dr. M. Kawano
The Division of Advanced Materials Science
Pohang University of Science and Technology (POSTECH)
San 31, Hyoja-dong, Pohang, 790-784 (South Korea)
E-mail: mkawano@postech.ac.kr
Homepage: http://mk.postech.ac.kr/

[**] This research was supported by WCU (World Class University) program (Project No. R31-2008-000-10059-0) and Basic Research (Project No. 2011-0009930) through the Korea Science and Engineering Foundation funded by the Ministry of Education, Science and Technology. This work was performed under the approval of the Photon Factory Program Advisory Committee (Proposal No. 2012G017) and Pohang Accelerator Laboratory (Proposal No. 2010-2086-04).

Supporting information for this article is available on the WWW under http://dx.doi.org/10.1002/anie.201306776.

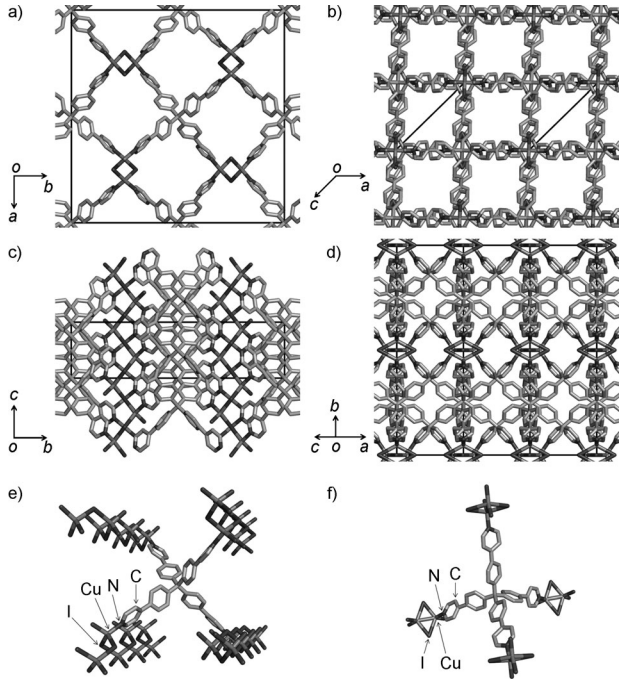

Figure 1. Porous network structure and coordination geometry of CuI unit in isomer **3a** (a,c,e) and **3b** (b,d,f). a,b) Packing structures viewed from the 1D channel (the *c* axis projection of isomer **3a** (a), the *b* axis projection of isomer **3b** (b)). c,d) Packing structures viewed from the direction perpendicular to the 1D channel (the *a* axis projection of isomer **3a** (c), the projection viewed from [102] direction of isomer **3b** (d)). e,f) Coordination geometries between the CuI unit (CuI helical chain unit in isomer **3a** (e), and Cu_2I_2 dimer unit in isomer **3b** (f)) and ligand **2**. Hydrogen atoms and solvent molecules are omitted for clarity.

described as a 4,4-connected network of PtS-type topology[9] considering the Cu_2I_2 dimer units as a square-planar site and the central carbon atom of the ligand **2** as the tetrahedral node. This structural topology is the same as that of the network consisting of Cu^{II} ions and the same ligand **2**.[7] The network isomer **3b** has 1D channels with a pore window of 4.0×3.9 Å and 22% void space in the unit cell volume. No Cu_2I_2 dimer units are facing to the channels.

Because the void space of isomer **3a** is larger than that of isomer **3b**, it is very likely that isomer **3a** is thermodynamically less stable than isomer **3b**. In fact, when kept in DMSO at 373 K for 1 day, all the yellow needle crystals of isomer **3a** were completely converted into orange prism crystals of isomer **3b** as was confirmed by X-ray diffraction analysis. After this conversion, even though the temperature of a DMSO solution containing isomer **3b** was increased to 462 K, the orange crystals never returned to the initial yellow crystals. It means that the network transformation process is irreversible. These facts indicate that isomer **3a** is the kinetic network and isomer **3b** is the thermally more stable network under these conditions.

Interestingly, the crystals of isomer **3a** are quite stable in the solid state, unlike in solution. The thermal stabilities of isomers **3a** and **3b** were investigated by thermogravimetric (TG) analysis. TG curves of isomer **3a** and **3b** showed weight loss corresponding to solvent evaporation at 300–520 K and 340–530 K, respectively, and decomposition above 673 K (see Figure S5). Even after the desolvation, crystals of **3a** and **3b** retained their crystallinity. These results indicate high robustness of the frameworks in the solid state. Using synchrotron X-ray diffraction, we also determined the structures of the desolvated crystals (isomer **3a′** from isomer **3a**, and isomer **3b′** from isomer **3b**) prepared by keeping the samples under vacuum at 423 K for 1 h. In the desolvated crystals **3a′** and **3b′**, the pyridyl and phenyl groups show disorder unlike in the solvated isomers **3a** and **3b**. Furthermore, the framework connectivity of the desolvated isomer **3b′** is different from that of the initial isomer **3b**. Half of the dimer unit are orthogonally rotated around the *a* axis on desolvation without ligand rearrangement (Figure S6).[10]

These network isomers show a unique sorption behavior of I_2. The I_2 sorption was monitored with sample weight change (Figure 2; and see Movie S1 and Figure S7 in the Supporting Information). A crystal of each of **3a**, **3a′**, **3b**, and **3b′** was put together with solid iodine on a dimpled slide glass capped by a flat slide glass at 293 K. The direction of 1D channel in all the crystals is along the long axis of the crystals. A solvated crystal of isomer **3a** and a desolvated crystal of isomer **3a′** turned black within 21 min and 3 min, respectively. The crystal structure analysis of the desolvated crystal of isomer **3a′** exposed to iodine vapor for 1 day gave a formulation as $(\mathbf{3a'}\cdot 0.96\,I_2)_n$. The diffraction became better after I_2 sorption (the maximum resolution of X-ray diffraction changed from 0.91 Å to 0.75 Å). The crystal-structure analysis revealed that the pores of solvated isomer **3a** and desolvated isomer **3a′** encapsulated I_2 by chemisorption through the formation of an I_3^- group from each bridging iodide unit giving a reasonable geometry for the I_3^- ion (Figure 3a; I1–I2 2.874(4) Å, I2–I3 2.800(8) Å, I1-I2-I3 angle: 175.9(3)°).[11] The intermolecular distance between I_3^- groups in a channel is 4.71(2) Å, indicating that there is no interaction between them.

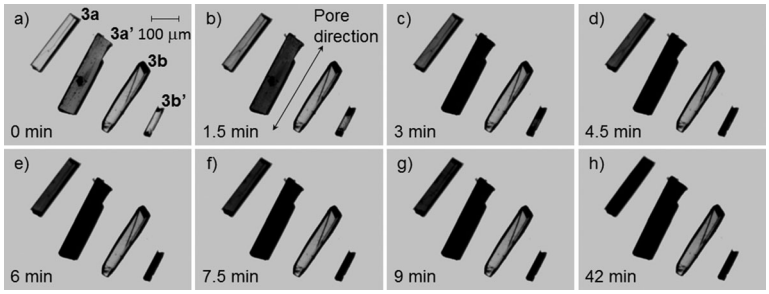

Figure 2. Photographs showing the iodine adsorption behavior of isomer **3a**, **3a′**, **3b**, and **3b′** (from left to right; see movie in Supporting Information) on exposing a single crystal of the isomer to iodine vapor. The crystals change color to black, except isomer **3b**.

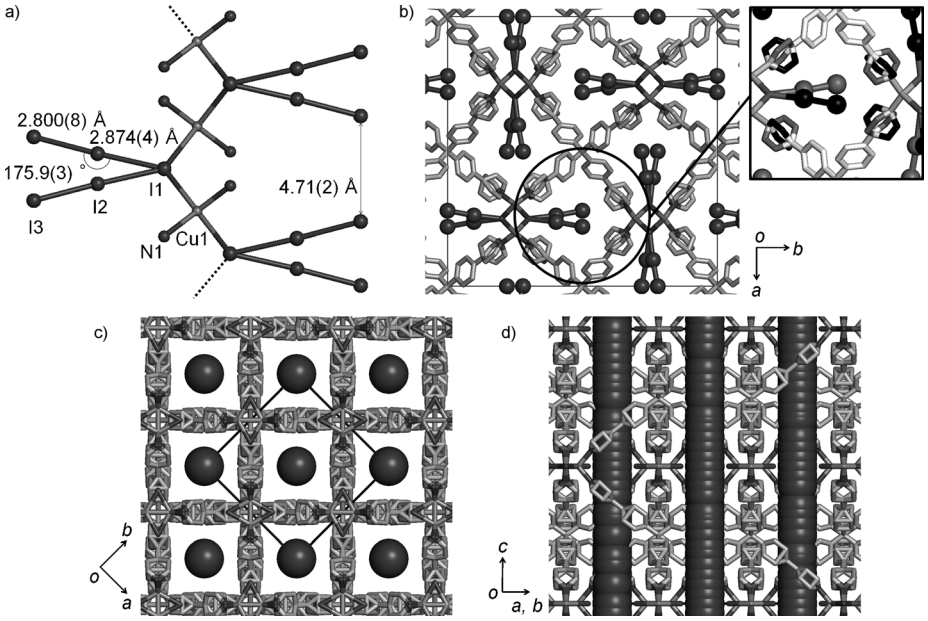

Figure 3. Structure of iodine-encapsulating network isomer **3a′** and **3b′**. a) A CuI helical chain unit with chemisorbed iodine molecules in iodine-encapsulating network isomer **3a′**. b) the *c*-axis projection of iodine-encapsulating network isomer **3a′** (Inset: differently shaded pairs of iodine molecules and pyridine rings belong to the same disordered pair). c,d) The physisorbed iodine in the iodine-encapsulating network isomer **3b′** c) the *c*-axis projection and d) the projection viewed from [110] direction. Hydrogen atoms and solvent molecules are omitted for clarity.

The desolvated network isomer **3b′** shows physisorption of I_2: the desolvated crystals of isomer **3b′** turned black within 5 min, giving $(\mathbf{3b'}\cdot 2.125\,I_2)_n$ (by X-ray analysis). The crystal-structure analysis revealed that I_2 molecules are arranged linearly along the 1D channels and highly disordered (Figure 3c,d).[12] Moreover, compared with $(\mathbf{3a'}\cdot 0.96\,I_2)_n$, $(\mathbf{3b'}\cdot 2.125\,I_2)_n$ shows a remarkable affinity for I_2: the I_2 desorption temperature in the TG measurement is 380 K for $(\mathbf{3a'}\cdot 0.96\,I_2)_n$ and 450 K for $(\mathbf{3b'}\cdot 2.125\,I_2)_n$ (see Figure S5). The large desorption temperature difference can be explained by steric repulsion between adsorbed I_2 molecules and the framework. Because the crystal structures of desolvated isomer **3a′** and isomer **3b′** at 80 K show severe disorder of phenyl and pyridyl rings, it is reasonable to assume that at higher temperatures these rings can rotate freely. Network $(\mathbf{3b'}\cdot 2.125I_2)_n$ has no steric hindrance with encapsulated I_2 molecules even though there is dynamic rotation of the rings at higher temperatures. However, in the case of $(\mathbf{3a'}\cdot 0.96\,I_2)_n$ severe collisions can occur between adsorbed I_2 molecules and the rotating pyridine rings (Figure 3b). Therefore, $(\mathbf{3a'}\cdot 0.96\,I_2)_n$ shows smooth desorption of I_2 over 380 K even though this sorption is chemisorption. Furthermore, the pore window of isomer **3b′** (4.0 × 3.9 Å) is exactly fit for iodine (the sum of van der Waals radii of iodine, 3.96 Å). That is why the physisorbed I_2 can be retained in the pore up to 450 K through the capillary effect.

On the adsorption of I_2, the crystal color of isomer **3a** and **3a′** changed almost uniformly (Figure 2; and see Movie S1 in the Supporting Information). This feature indicates that I_2 molecules were adsorbed not only by the 1D channel but also by cracks and defects on the surface of the crystal. It is reasonable to assume that kinetic networks have more defects than thermodynamic networks. Once the I_3^- group forms, the 1D channel is blocked. Therefore, subsequent I_2 molecules cannot enter the channel as long as the I_3^- group is blocking the channel. However, covalent bond formation is energetically favorable, therefore I_2 molecules were adsorbed through cracks and defects on the surface of the crystal to form more I_3^- groups in the channels. Also, we observed the creation of new cracks on the surface of a solvated crystal of isomer **3a** during I_2 sorption. Crystal solvents cannot escape through the channel owing to the blocking I_3^- group, but they can escape by creation of new cracks on the surface.

In contrast to isomer **3a** and **3a′**, a desolvated crystal of isomer **3b′** gradually adsorbed I_2 from the edge of the channel. Because of physisorption, I_2 molecules just diffused into the channel. In the case of solvated form isomer **3b**, I_2 molecules cannot enter the channel, because crystal solvent, DMSO, is tightly encapsulated. Indeed, DMSO encapsulated in isomer **3b** cannot be removed at room temperature in vacuo. According to the TG results for isomer **3b**, we needed to heat the crystals over 340 K to remove the crystal solvent. It is of note that the desolvated form isomer **3b′** could not go back to solvated form isomer **3b** on immersing it in DMSO at room temperature, but it could at 373 K. These facts indicate that the bulky molecule larger than the pore window size (ca. 4.0 Å) cannot easily enter the quadruply interpenetrated network isomer **3b′**, and contribute to the physisorption process in isomer **3b′**.

To monitor the weight change of desolvated isomer **3a′** and **3b′** on the adsorption of I_2, the crystals of isomer **3a′**, **3b′**, and iodine solid were put in vials separately, then the three vials were put in a bigger vial together. After the bigger vial was capped, the weights of smaller vials were measured from time to time (see Figure S7). After the I_2 sorption, 110 wt% and 58 wt% increase were found on the basis of the initial mass in isomer **3a′** and **3b′**, respectively. The ideal maximum capacity for encapsulation of I_2 into both isomers is 50 wt% (two I_2 molecules can be encapsulated per each network unit as $\{[(CuI)_2(\mathbf{2})]\cdot 2\,I_2\}_n$. The excess mass increase compared with the ideal maximum capacity suggests continuous deposition onto the surface of both crystals. To remove excess iodine on the surface of the crystals, the crystals were washed with cyclohexane. In both cases, the mass increase of the washed crystals were 45 wt%, indicating 90% pore spaces are occupied by encapsulated iodine molecules. This value is comparable to the value of other porous coordination networks.[5]

I_2 adsorption was further tested using I_2 solution. When the crystals of isomer **3a′** or **3b′** were immersed in a purple cyclohexane solution of I_2, the color gradually faded, indicating that iodine was encapsulated into the networks in solution as well. Therefore, we investigated these encapsulation processes in cyclohexane with UV/Vis spectroscopy. The kinetic analyses reveal the chemisorption of isomer **3a′** and physisorption of isomer **3b′**. The absorbance decreased on the adsorption of I_2 (see Figure S1 and S2). The adsorption kinetics were investigated by monitoring the 525 nm absorbance (see Insets of Figure S1 and S2). In adsorption kinetics, the plot of time versus $\ln(A_t - A_\infty)$ should be linear for a first-order reaction and plot of time versus time/$(A_0 - A_t)$ should be linear for a second-order reaction (A_0: initial absorbance, A_t: absorbance at time t, A_∞: absorbance at equilibrium).[13] The sorption of I_2 by isomer **3b′** followed first-order reaction kinetics: the rate constant of adsorption was determined as $4.7 \times 10^{-3}\ \mathrm{min}^{-1}$. On the other hand, the sorption of I_2 by isomer **3a′** can be described by two steps: a first-order reaction (reaction rate: $1.6 \times 10^{-3}\ \mathrm{min}^{-1}$) followed by a second-order reaction (reaction rate: 159 g(sorbent)/(mg(solute)·min), see Insets of Figure S2). This result suggests that the first step until approximately 360 min is dominated by physisorption, however, the second step from approximately 360 min is a competitive reaction between physisorption and I_3^- bond formation/cleavage. At approximately 360 min, around 10% of pore was filled by I_2 (calculated from the I_2 concentration determined by the absorption value). From this moment, even though I_2 has not filled the pore entirely, the chemisorption process becomes the rate-limiting step.

To clarify the network formation mechanism of isomer **3a** and **3b** in DMSO, we investigated a colorless reaction solution of **1** and **2** by NMR spectroscopy. The NMR study demonstrated that network formation requires oxygen during the reaction. In the absence of oxygen, no reaction proceeded, resulting in no network crystal formation. Therefore, it is intriguing to know what the reaction intermediate for networking is. To reveal the intermediate species, right after mixing **1** and **2** in [D_6]DMSO in a NMR tube in air at 453 K for 30 min in an oil bath, we measured ^{1}H NMR of the reaction solution at 400 K (the highest probe temperature we could reach). The NMR spectrum showed that the resonance signals of the pyridyl group in ligand **2** shifted downfield with broadening of the signal for the α-proton and retention of T_d symmetry (Figure S8 a,b). The result indicates that the intermediate species has a Cu−N coordination bond and T_d symmetry. Another important fact is that signals for O=PPh_3 were observed at around δ = 7.50–7.65 ppm (Figure S8 c). As a control experiment, the network synthesis was performed under Ar by using a degassed DMSO solution. Unexpectedly, although a colorless solution was obtained after heating at 453 K, no crystals were obtained by cooling the solution. Similarly to the above experiment in air, the ^{1}H NMR measurement was performed under Ar. As we expected, no signals for O=PPh_3 were found. The observed signals exactly matched those of the starting materials, **1** and **2**, indicating that the starting materials were still present just as mixture under Ar (Figure S9). Therefore, NMR spectroscopic and X-ray results suggest the following possible networking mechanism: firstly, the PPh_3 group of starting material **1** was removed by oxidation to produce a vacant site; secondly, the vacant site on a copper atom can be coordinated by DMSO and simultaneously solvated CuI monomer may be generated at 453 K. Then ligand **2** coordinates to the CuI monomer to generate the intermediate species, {[CuI(DMSO)$_2$]$_4$(**2**)}.[14] When the reaction was performed at 433 K in air, the CuI helical chain network isomer **3a** was not obtained as a major product even by rapid cooling, indicating that the CuI monomer can be generated as a major species in the reaction solution above 453 K. Because the Cu_2I_2 dimer is thermodynamically more stable than the CuI helical chain, at temperatures below 453 K or on slow cooling from 453 K, the Cu_2I_2 dimer network isomer **3b** can be obtained selectively.

We have successfully demonstrated the kinetic control of network formation using labile metal sources. We could obtain two kinds of networks, isomer **3a** and **3b**, which are thermally stable. The network formation mechanism was confirmed by NMR spectroscopy. Both networks show unique I_2 sorption properties. Using kinetic control, we could arrange bridging iodides facing into a pore in isomer **3a** to enable chemisorption of I_2. Compared with isomer **3b**, isomer **3a** can be also useful for application, because isomer **3a** can efficiently absorb/desorb I_2 by temperature control. The I_2 chemi-/physi- sorption process of these networks were also clarified by kinetic measurements in solution. Another important message of this study is that, even using kinetic control, thermally stable porous networks in the solid state can be obtained. We believe that kinetic control can be a useful synthetic strategy to create a new class of porous materials.

Received: August 2, 2013
Published online: September 25, 2013

Keywords: chemisorption · copper · iodine · metal–organic frameworks · physisorption

[1] a) S. R. Batten, R. Robson, *Angew. Chem.* **1998**, *110*, 1558–1595; *Angew. Chem. Int. Ed.* **1998**, *37*, 1460–1494; b) M. Eddaoudi, D. B. Moler, H. Li, B. Chen, T. M. Reineke, M. O'Keeffe, O. M. Yaghi, *Acc. Chem. Res.* **2001**, *34*, 319–330; c) B. Moulton, M. J. Zaworotko, *Chem. Rev.* **2001**, *101*, 1629–1658; d) S. Kitagawa, R. Kitaura, S. Noro, *Angew. Chem.* **2004**, *116*, 2388–2430; *Angew. Chem. Int. Ed.* **2004**, *43*, 2334–2375; e) G. Férey, *Chem. Soc. Rev.* **2008**, *37*, 191–214; f) B. D. Chandler, G. D. Enright, K. A. Udachin, S. Pawsey, J. A. Ripmeester, D. T. Cramb, G. K. H. Shimizu, *Nat. Mater.* **2008**, *7*, 229–235; g) T. Yamada, H. Kitagawa, *J. Am. Chem. Soc.* **2009**, *131*, 6312–6313; h) N. F. Sciortino, K. R. Scherl-Gruenwald, G. Chastanet, G. J. Halder, K. W. Chapman, J.-F. Létard, C. J. Kepert, *Angew. Chem.* **2012**, *124*, 10301–10305; *Angew. Chem. Int. Ed.* **2012**, *51*, 10154–10158; i) S. J. Geier, J. A. Mason, E. D. Bloch, W. L. Queen, M. R. Hudson, C. M. Browncd, J. R. Long, *Chem. Sci.* **2013**, *4*, 2054–2061.

[2] a) S. Noro, S. Kitagawa, T. Akutagawa, T. Nakamura, *Prog. Polym. Sci.* **2009**, *34*, 240–279; b) F. A. Almeida Paz, J. Klinowski, S. M. F. Vilela, J. P. C. Tomé, J. A. S. Cavaleiro, J. Rocha, *Chem. Soc. Rev.* **2012**, *41*, 1088–1110.

[3] a) M. Kawano, T. Haneda, D. Hashizume, F. Izumi, M. Fujita, *Angew. Chem.* **2008**, *120*, 1289–1291; *Angew. Chem. Int. Ed.*

2008, *47*, 1269 – 1271; b) K. Ohara, J. Martí-Rujas, T. Haneda, M. Kawano, D. Hashizume, F. Izumi, M. Fujita, *J. Am. Chem. Soc.* **2009**, *131*, 3860 – 3861; c) J. Martí-Rujas, Y. Matsushita, F. Izumi, M. Fujita, M. Kawano, *Chem. Commun.* **2010**, *46*, 6515 – 6517; d) J. Martí-Rujas, N. Islam, D. Hashizume, F. Izumi, M. Fujita, M. Kawano, *J. Am. Chem. Soc.* **2011**, *133*, 5853 – 5860; e) J. Martí-Rujas, N. Islam, D. Hashizume, F. Izumi, M. Fujita, H. J. Song, H. C. Choi, M. Kawano, *Angew. Chem.* **2011**, *123*, 6229 – 6232; *Angew. Chem. Int. Ed.* **2011**, *50*, 6105 – 6108; f) Y. Yakiyama, A. Ueda, Y. Morita, M. Kawano, *Chem. Commun.* **2012**, *48*, 10651 – 10653; g) J. Martí-Rujas, M. Kawano, *Acc. Chem. Res.* **2013**, *46*, 493 – 505.

[4] a) B. J. Hathaway in *Comprehensive Coordination Chemistry*, *Vol. 5* (Eds.: G. Wilkinson, R. D. Gillard, J. A. McCleverty), Pergamon, Oxford, **1987**, pp. 533 – 774; b) K. Ohara, K. Yamaguchi, *Anal. Sci.* **2012**, *28*, 635 – 637.

[5] a) D. F. Sava, M. A. Rodriguez, K. W. Chapman, P. J. Chupas, J. A. Greathouse, P. S. Crozier, T. M. Nenoff, *J. Am. Chem. Soc.* **2011**, *133*, 12398 – 12401; b) K. W. Chapman, P. J. Chupas, T. M. Nenoff, *J. Am. Chem. Soc.* **2010**, *132*, 8897 – 8899; c) M.-H. Zeng, Q.-X. Wang, Y.-X. Tan, H.-X. Zhao, L.-S. Long, M. Kurmoo, *J. Am. Chem. Soc.* **2010**, *132*, 2561 – 2563; d) J.-P. Lang, Q.-F. Xu, R.-X. Yuan, B. F. Abrahams, *Angew. Chem.* **2004**, *116*, 4845 – 4849; *Angew. Chem. Int. Ed.* **2004**, *43*, 4741 – 4745; e) Z. Yin, Q.-X. Wang, M.-H. Zeng, *J. Am. Chem. Soc.* **2012**, *134*, 4857 – 4863; f) T. Hasell, M. Schmidtmann, A. I. Cooper, *J. Am. Chem. Soc.* **2011**, *133*, 14920 – 14923; g) K. W. Chapman, D. F. Sava, G. J. Halder, P. J. Chupas, T. M. Nenoff, *J. Am. Chem. Soc.* **2011**, *133*, 18583 – 18585; h) D. F. Sava, T. J. Garino, T. M. Nenoff, *Ind. Eng. Chem. Res.* **2012**, *51*, 614 – 620; i) Z.-M. Wang, Y.-J. Zhang, T. Liu, M. Kurmoo, S. Gao, *Adv. Funct. Mater.* **2007**, *17*, 1523 – 1536; j) L. Dotrzańska, G. O. Lloyd, H. G. Raubenheimer, L. J. Barbour, *J. Am. Chem. Soc.* **2006**, *128*, 698 – 699; k) B. F. Abrahams, M. Mylan, S. D. Orchard, R. Robson, *Angew. Chem.* **2003**, *115*, 1892 – 1895; *Angew. Chem. Int. Ed.* **2003**, *42*, 1848 – 1851; l) C. H. Görbitz, M. Nilsen, K. Szeto, L. W. Tangen, *Chem. Commun.* **2005**, 4288 – 4290; m) L. Mohanambe, S. Vasudevan, *Inorg. Chem.* **2004**, *43*, 6421 – 6425; n) H. J. Choi, M. P. Suh, *J. Am. Chem. Soc.* **2004**, *126*, 15844 – 15851.

[6] a) J. C. Dyason, P. C. Healy, L. M. Engelhardt, C. Pakawatchai, V. A. Patrick, C. L. Raston, A. H. White, *J. Chem. Soc. Dalton Trans.* **1985**, 831 – 838; b) R.-Z. Li, D. Li, X.-C. Huang, Z.-Y. Qi, X.-M. Chen, *Inorg. Chem. Commun.* **2003**, *6*, 1017 – 1019; c) E. Cariati, D. Roberto, R. Ugo, P. C. Ford, S. Galli, A. Sironi, *Inorg. Chem.* **2005**, *44*, 4077 – 4085.

[7] C. B. Caputo, V. N. Vukotic, N. M. Sirizzotti, S. J. Loeb, *Chem. Commun.* **2011**, *47*, 8545 – 8547.

[8] A porous network structure based on an infinite CuI zigzag chain has been reported: S. Q. Liu, H. Konaka, T. Kuroda-Sowa, Y. Suenaga, H. Ito, G. L. Ning, M. Munakata, *Inorg. Chim. Acta* **2004**, *357*, 3621 – 3631.

[9] M. O'Keeffe, M. Eddaoudi, H. Li, T. Reineke, O. M. Yaghi, *J. Solid State Chem.* **2000**, *152*, 3 – 20.

[10] We will report the dynamic motion of the dimer unit elsewhere.

[11] a) J. Runsink, S. S. -Walstra, T. Migchelsen, *Acta Crystallogr. Sect. B* **1972**, *28*, 1331 – 1335; b) K.-F. Tebbe, B. Freckmann, M. Hörner, W. Hiller, J. Strähle, *Acta Crystallogr. Sect. C* **1985**, *41*, 660 – 663; c) K.-F. Tebbe, U. Georgy, *Acta Crystallogr. Sect. C* **1986**, *42*, 1675 – 1678; d) P. H. Svensson, L. Kloo, *Chem. Rev.* **2003**, *103*, 1649 – 1684.

[12] Organic zeolite, a phosphazene crystal that has channels with a diameter of about 5 Å shows a similar I_2 physisorption behavior: a) H. R. Allcock, L. A. Siegel, *J. Am. Chem. Soc.* **1964**, *86*, 5140 – 5144; b) T. Hertzsch, F. Budde, E. Weber, J. Hulliger, *Angew. Chem.* **2002**, *114*, 2385 – 2388; *Angew. Chem. Int. Ed.* **2002**, *41*, 2281 – 2284.

[13] a) Y. S. Ho, G. McKay, *Process Biochem.* **1999**, *34*, 451 – 465; b) C. Chen, M. Zhang, Q. Guan, W. Li, *Chem. Eng. J.* **2012**, *183*, 60 – 67.

[14] In this reaction, NMR and ESR results suggest that the oxidation state of copper is always + I.

